DESIGN OF A PRECISION FERTILIZATION CONTROL SYSTEM BASED ON THE DE-PID ALGORITHM
/
基于 DE-PID 算法的精准施肥控制系统设计

Xuan LUO, He SUN, Xiaoliang LI, Xinlin LI, Yue SHI, Yihui MIAO, Haoran BAI*)
College of Mechanical and Electrical Engineering, Qingdao Agricultural University Qingdao /China
Tel: +86 13854285625; E-mail: baihaoran111@126.com
Corresponding author: Haoran BAI
DOI: https://doi.org/10.35633/inmateh-78-65

Keywords: *Closed-loop Control, Stepper Motor, Differential Evolution Optimization, Fertilizer Uniformity, Agricultural Automation, PID Tuning*

ABSTRACT
To address issues related to fertilization accuracy and uniformity under field conditions affected by terrain undulations and load fluctuations, an electric precision fertilization control system based on a Siemens S7-200 SMART PLC was developed. The system employs a stepper motor as the actuator and incorporates an incremental encoder with 2,000 pulses per revolution to provide closed-loop speed feedback. A PID parameter optimization method based on differential evolution (DE) is proposed, which performs global optimization using fitness functions defined by tracking error and dynamic performance. Comparative simulations of DE-PID and conventional PID were conducted in MATLAB, followed by field experiments in Dongying City, Shandong Province. The results show that, under conventional PID control, the maximum relative error, average relative error, and coefficient of variation were 4.2%, 3.68%, and 0.36%, respectively, whereas under DE-PID control, these values decreased to 3.2%, 2.92%, and 0.23%, respectively. These findings indicate that the DE-PID strategy effectively improves fertilization accuracy and uniformity, providing a reference for the precise control of external-grooved wheel-type fertilization equipment.

摘要
针对受地面起伏和负载波动影响的田间条件下，外槽轮施肥机的施肥精度和均匀性，开发了一种基于西门子 S7-200 SMART PLC 的电动精密施肥控制系统。该系统采用步进电机作为执行器，并使用 2000 脉冲/转的增量编码器建立闭环速度反馈。本文提出了一种基于差分进化（DE）的 PID 参数优化方法，通过基于跟踪误差和动态性能的适应度函数进行全局优化。在 MATLAB 中对 DE-PID 与传统 PID 进行了对比仿真，并在山东省东营市进行了现场试验。结果表明，在传统 PID 控制下，最大相对误差、平均相对误差和变异系数分别为 4.2%、3.68%和 0.36%，而在 DE-PID 控制下，这些指标分别降至 3.2%、2.92%和 0.23%。结果表明，DE-PID 策略可有效提高施肥精度和均匀度，为外槽轮式施肥设备的精准控制提供了参考。

INTRODUCTION
Precision fertilization is an important technological approach for achieving green and efficient agricultural production as well as reducing fertilizer inputs while improving nutrient use efficiency. Its core principle is to realize quantitative and accurate fertilizer application according to spatial variability in soil nutrients, crop nutrient demand patterns, and target yield requirements *(Nan et al., 2024; Sharaby et al., 2019).* Conventional fertilization equipment typically relies on mechanical metering or simplified electronic control, and commonly suffers from insufficient regulation accuracy of application rate, strong susceptibility to ground undulation and load fluctuations during operation, and sluggish dynamic response. These issues lead to increased errors in fertilizer application per unit area and reduced application uniformity, thereby causing fertilizer waste and decreasing crop nutrient utilization efficiency *(Deng et al., 2019; Han et al., 2024).* Therefore, developing a high-precision precision-fertilization control system for complex field conditions is of great significance for improving fertilization quality. As a result, the relationship between discharge rate and roller rotational speed exhibits certain nonlinearity and time-varying characteristics. When an open-loop control strategy is adopted, it is difficult to simultaneously ensure satisfactory dynamic response and steady-state stability under different target application rates and varying load conditions *(Boac et al., 2014; Zhang et al., 2021)*.

This often leads to overshoot in fertilizer discharge and increased steady-state fluctuations, ultimately deteriorating the unit-time discharge error and application uniformity.

To address these issues, this study developed an electrically driven precision fertilization control system for a fluted-roller fertilizer applicator based on a Siemens S7-200 SMART controller. In terms of control strategy, given that conventional PID tuning relies heavily on experience and is difficult to adapt to complex operating conditions, a Differential Evolution (DE)–based PID parameter optimization method was proposed *(Wang et al., 2017; Umeda et al., 2001)*. A performance index centered on tracking error and dynamic characteristics was constructed to achieve global optimization and tuning of PID parameters. Finally, field experiments were conducted to verify the unit-time fertilizer discharge error and fertilization uniformity of the proposed system, providing a reference for improving the precision and intelligence of fluted-roller fertilization equipment *(Huang et al., 2024; Zhu et al., 2025)*. In response to this problem, some researchers have explored various precision control solutions. Chen Man et al. designed an intelligent precision seeding–fertilizing control system for winter wheat; the system adopted a speed-measurement method and PWM control to monitor and regulate the fertilizer-metering motor speed in real time, thereby achieving precision seeding and fertilization *(Huang et al., 2025; Zhu et al., 2024)*. Umeda et al. developed a variable-rate fertilization machine for paddy fields; the machine relied on sensors to acquire ground-wheel speed data in real time and, together with a preset prescription map, enabled accurate control of fertilizer discharge for each grid unit in the paddy field. Building on these studies, this work designed an electrically driven precision fertilization control system.

The system uses a stepper motor as the actuator and establishes a mathematical motor model to analyze the dynamic performance of the control system. Tuning was performed using the DE-PID algorithm. Through simulation, the feasibility of the control system was verified using metrics such as rise time, peak time, overshoot, and steady-state error of the response curve. In addition, field tests were conducted to evaluate the actual control performance under different operating conditions based on real-world control accuracy and response speed, thereby providing theoretical support and experimental evidence for improving the electric precision fertilizer control system.

MATERIALS AND METHODS

Structure and Working Principle of the Fluted-Roller Fertilizer Applicator

The structure of the fluted-roller fertilizer applicator investigated in this study is shown in Fig. 1. The fluted-roller fertilizer applicator is one of the most widely used quantitative fertilizer metering devices in agricultural production. Its basic working principle involves a rotor with external flutes rotating within the fertilizer bed, conveying granular fertilizer to the discharge outlet according to the volume of the flute cells, and releasing it to achieve fertilizer delivery. Based on the conventional mechanical metering mechanism, the precision fluted-roller fertilization system developed in this study incorporates an electric drive and a closed-loop control unit. The overall structure can be divided into three subsystems: the control system, the actuation unit, and the fertilizer metering and discharge mechanism.

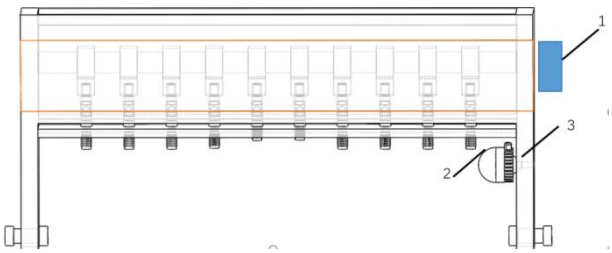

Fig. 1 – Schematic diagram of the fluted-roller fertilizer applicator

1 - Control System; 2 - Executive body; 3 - Fertilizer Application Mechanism

The control system of the fluted-roller fertilizer applicator mainly consists of an incremental encoder, a Siemens S7-200 SMART PLC, a stepper motor, and the corresponding stepper driver. The operating principle of the system is shown in Fig. 2.

During field operation, the fertilizer applicator is towed forward by a tractor. The incremental encoder is mounted on the stepper motor shaft to acquire the motor speed in real time. In operation, the controller calculates the target roller speed according to the preset fertilizer application rate and drives the stepper motor accordingly.

When the roller rotates in the working zone beneath the hopper, the fluted cells enter the fertilizer bed and are filled with granules. As the roller continues to rotate, the filled cells move to the discharge outlet, where the fertilizer is released under gravity and inertia and delivered into the soil through the delivery tube. Meanwhile, the incremental encoder continuously feeds the shaft rotation information back to the PLC. The PLC periodically computes the actual speed and compares it with the target value to obtain the speed error. The PID controller then generates a control action based on this error to adjust the pulse frequency, thereby maintaining stable roller speed even in the presence of disturbances such as load fluctuations and changes in fertilizer flowability. As a result, the unit-time discharge error is reduced and fertilizer application uniformity is improved.

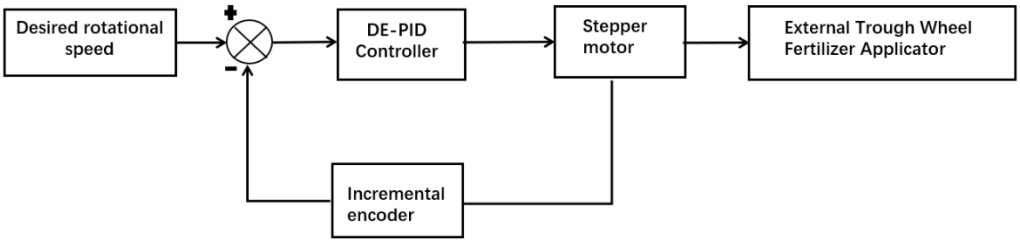

Fig. 2 – Working principle of the fluted-roller fertilizer applicator

Control System Design and Mathematical Modeling

The PLC controls the stepper motor by using high-speed pulse outputs to drive the PUL and DIR terminals of the MA860 stepper driver *(He et al., 2018; Zubrilina et al., 2019).* A high-speed counter (HSC) is employed to read the encoder pulse count within a sampling period of 100 ms. The system uses SM0.1 to call the initialization subroutine at power-on and SM0.0 to invoke the interrupt routine. Because the Siemens S7-200 SMART ST40 controller cannot modify the output frequency while the PLS instruction is being executed (the frequency can only be changed after pulse transmission is completed or after a forced stop), the stepper motor is driven using the motion control (wizard-based) instruction set instead of the PLS instruction. The subroutine is used to configure/enable the high-speed counter, and the interrupt routine is used to read the pulse count from the high-speed counter. The main program structure is partially illustrated in Fig. 3.

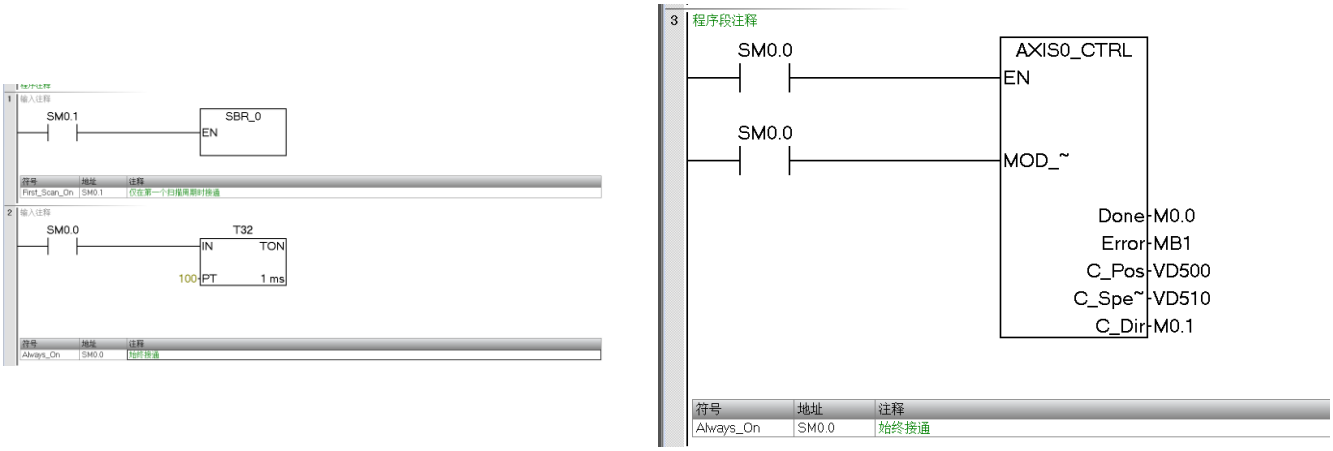

Fig. 3 – Partial Main Program Diagram

The rotational speed measurement and calculation are described in Eq. (1). The rotational speed of the stepper motor is determined by the input pulse frequency. With the driver configured to a microstepping resolution corresponding to 1600 pulses per revolution, the motor speed can be accurately controlled. A closed-loop control system is established by mounting an incremental encoder on the shaft of the fluted roller. The encoder provides 2000 pulses per revolution for feedback.

$$n = \frac{f}{2000} \times 60 \quad (1)$$

where: n - represents the rotational speed of the stepper motor [r/min];

f - represents the number of pulses collected by the encoder [D].

Mathematical model

In this study, a transfer function model of the control system was established *(Hou et al., 2023; Inthiyaz et al., 2021)*. An 86BYG250H stepper motor was selected as the actuator. The basic architecture of the PID control system comprises three core components: the controller module, the actuation unit, and the feedback sensing unit, as illustrated in Fig. 4. Specifically, the controller module performs the control algorithm computations, the actuation unit executes the control actions, and the feedback sensing unit monitors the system state in real time and provides feedback for closed-loop regulation.

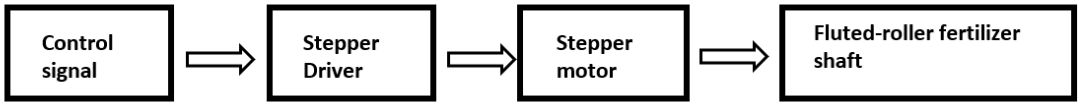

Fig. 4 – Block diagram of the PID control system

The single-phase equivalent circuit of a two-phase hybrid stepper motor is shown in Figure 5.

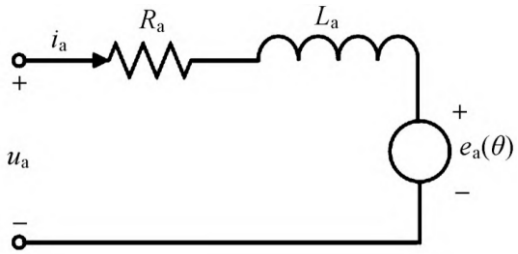

Fig. 5 – Single-Phase Equivalent Circuit Diagram of a Two-Phase Hybrid Stepper Motor

The parameters of the stepper motor studied in this paper are shown in Table 1.

Table 1

Stepper Motor Parameter Table

Parameter Name	Parameter value
Phase current / A	4.2
Mutual Inductance / mH	3.5
Moment of inertia / kg.cm^2	2.7
Viscosity coefficient / D	0.25
Number of rotor teeth / Zr	50

Proportional component of the drive section:

$$G_1(s)=\frac{U_{out}}{U_{in}}=Ks=2 \quad (2)$$

In the equation: $G_1(s)$ is the transfer function of the driver stage. G is the general symbol for the transfer function; the subscript 1 corresponds to the first stage of the system (the driver stage); s is the Laplace operator.Uin is the input to the drive section, i.e., the control signal voltage applied to the stepper motor driver.Uout is the output of the drive section, i.e., the operating voltage supplied by the driver to the stepper motor windings.Ks is the proportional gain of the drive section; here, its value is determined by circuit parameters to be 2.

The selected stepper motor is a two-phase hybrid stepper motor. By establishing a mathematical model based on the physical characteristics of this type of stepper motor, the back EMF for phases A and B is obtained as follows:

$$U_A=K\,\omega\,sin(Z\theta) \quad (3)$$

$$U_B=K\,\omega\,sin(Z\theta-\pi) \quad (4)$$

In the equation: K is the motor torque constant; ω is the angular velocity of the rotor; Z is the number of teeth; θ is the mechanical angle of the rotor. According to Ohm's law, the phase voltages A and B can be calculated as follows:

$$V_A = \frac{dI_A}{dt}L + \frac{dI_B}{dt}L_M + RI_A - K\omega sin(Z\theta) \quad (5)$$

$$V_B = \frac{dI_B}{dt}L + \frac{dI_A}{dt}L_M + RI_B - K\omega sin(Z\theta - \pi) \quad (6)$$

In Equations 5 and 6: L is the mutual inductance between phases A and B; L_m is the mutual inductance between motor windings; R is the resistance; I_A and I_B are the currents of phases A and B, respectively; dI_A/t and dI_B/t are the rates of change of current in phases A and A, respectively.

If the motor torque remains constant, where Tm is the motor torque and ω = dθ/dt, then the equation of motion is:

$$T_m = J\frac{d\omega}{dt} + D_\omega + T_R \quad (7)$$

J is the rotational inertia of the motor; D is the braking damping coefficient; T_R is the load torque. D_ω is the dynamic resistance moment.

$$J(\frac{d\omega}{dt}d\omega/dt) + D_\omega + T_R = KI_A sin(Z\theta) + KI_B sin(Z\theta - \pi) \quad (8)$$

If the input to the stepper motor is the rotation angle θ_1 and the output is the actual rotation angle θ_2 of the motor, then the transfer function is:

$$G_s = \frac{\theta_{2(s)}}{\theta_{1(s)}} \quad (9)$$

When the torque of a stepper motor is zero, the motor is in an unloaded state, and its motion mode is:

$$J\frac{d\omega}{dt} + D\omega - \frac{Z^2LI^2A}{2}sin(Z\theta) = 0 \quad (10)$$

When θ is very small, then $\sin\theta = \theta$.

$$J\frac{d^2\theta_2}{dt^2} + D\frac{d\theta_2}{dt} - \frac{Z^2LI^2A}{2}(\theta 2 - \theta 1) \quad (11)$$

where I is the phase current, L is the mutual inductance, J is the moment of inertia, D is the viscosity coefficient, and Z is the number of rotor teeth. Applying the Laplace transform to Eq. (11), the following expression is obtained:

$$G_{2(s)} = \frac{\theta_{2(s)}}{\theta_{1(s)}} = \frac{\omega_{2(s)}}{\omega_{1(s)}} = \frac{Z^2L\,I^2A}{2J\,s^2 + 2D\,s + Z^2L\,I^2A} \quad (12)$$

It follows that the transfer function of the stepper motor is:

$$G_{2(s)} = \frac{155}{5.4\times10^{(-4)}s^2 + 0.5s + 155} \quad (13)$$

RESULTS AND DISCUSSIONS

Traditional PID Controller

As shown in Fig. 6, the PID controller is widely applied in motor speed regulation and the operational control of agricultural machinery due to its simple structure, clear physical interpretation of parameters, and ease of engineering implementation. For the fluted-roller fertilizer applicator, the control objective is to ensure that the roller speed stably tracks the target value, thereby reducing fluctuations in the fertilizer discharge rate and improving application uniformity. Based on the closed-loop control framework established above, the PID controller uses the speed error as the input and the stepper motor drive pulse frequency as the output, enabling real-time regulation of the actuator.

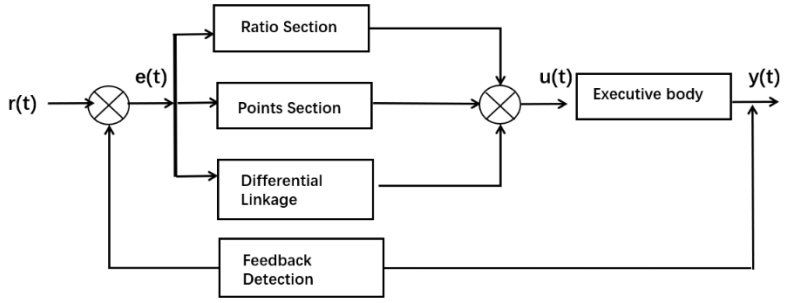

Fig. 6 – PID Controller Schematic Diagram

Based on the schematic diagram, the system deviation is as follows:

$$e(t) = r(t) - y(t) \tag{14}$$

The PID controller adjusts control parameters online based on system deviation, thereby generating control actions for the target system as follows:

$$u(t) = K_p e(t) + K_i \int_0^t e(\tau)d\tau + K_d \frac{de(t)}{dt} \tag{15}$$

By applying discretization and weighting to the integral term, the incremental PID formula can be derived:

$$\Delta u(k) = K_p(e(k) - e(k-1)) + K_i e(k) + K_d(e(k) - 2e(k-1) + e(k-2)) \tag{16}$$

In the equation: $r(t)$ represents the system input; $y(t)$ represents the system output. $C\_(t-1)$ denotes the control variable at time t; K_p is the proportional coefficient; K_i is the integral coefficient; K_d is the derivative coefficient.

DE-PID Controller

As shown in Fig. 7, the Differential Evolution (DE) algorithm is a population-based intelligent optimization method for continuous variables. It features a simple implementation, good convergence performance, and low requirements on the differentiability of the objective function *(Cao et al., 2022; Chen et al., 2022)*. In this study, the PID parameters were treated as decision variables, and the DE algorithm was used to perform iterative searches within predefined bounds to obtain an optimal parameter combination that satisfies both dynamic response and steady-state stability requirements, thereby forming a DE-PID controller. The overall procedure of the Differential Evolution algorithm is illustrated in Fig. 8.

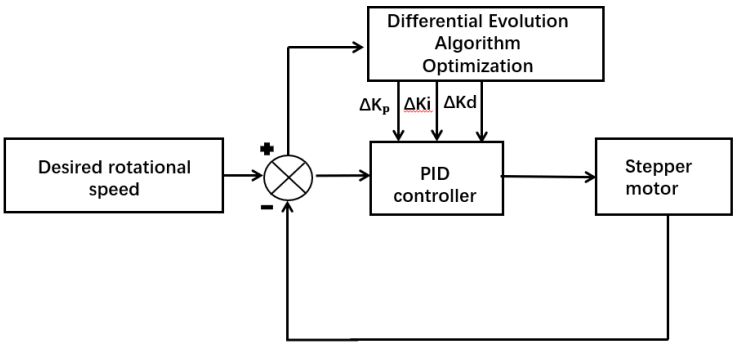

Fig. 7 – DE-PID Controller Structure

Individual encoding: A set of PID parameters is treated as an individual.

$$x = [Kp, Ki, Kd] \tag{17}$$

The population consists of NP individuals:

$$\{X_1, X_2, \ldots, X_{NP}\} \tag{18}$$

To prevent the algorithm from generating infeasible PID parameters and to avoid destabilizing the closed-loop system, while simultaneously reducing the search space and improving optimization efficiency, the following bounds are imposed on the PID parameters based on the electromechanical characteristics of the stepper motor and the speed control requirements of the fluted-roller system:

$$\begin{cases} K_p \in [K_{p,min}, K_{p,max}] = [0, 30] \\ K_i \in [K_{i,min}, K_{i,max}] = [0, 1] \\ K_d \in [K_{d,min}, K_{d,max}] = [0, 10] \end{cases} \tag{19}$$

The key to the DE-PID method lies in the design of the fitness function. The optimization objectives of this study include minimizing speed tracking error, achieving a fast dynamic response, reducing overshoot, minimizing steady-state fluctuations, and ensuring smooth control output. Accordingly, a comprehensive objective function is constructed as follows:

$$J = w_1 * ITAE + w_2 * M_p + w_3 * T_s + w_4 * u \quad (20)$$

where: J is the value of the composite objective function;

w_1, w_2, w_3, and w_4 are the weighting coefficients for each sub-performance metric, satisfying $w_1 + w_2 + w_3 + w_4 = 1$;

$ITAE$ is the time-weighted integral of absolute error;

M_p is the maximum overshoot of the system's step response;

T_s is the settling time of the system's step response;

u is the cumulative absolute value of the control increment.

$ITAE$ is a classic metric for evaluating the tracking performance of control systems. The discrete formula for $ITAE$ is:

$$ITAE = \sum_{k=1}^{N} \mathrm{k} * T * |ek| \quad (21)$$

where: k is the sample time index, where $k = 1, 2, \ldots..$;

N is the total number of simulation steps;

T is the sampling period; in this paper, $T = 0.1$ s;

$e(k)$ is the speed tracking error at time k;

$n_{out}(k)$ is the actual speed of the stepper motor at time k.

The weighting coefficients were determined based on the operational priorities of the fluted-roller fertilizer applicator under field conditions. Tracking accuracy ($w_1 = 0.5$) was assigned the highest weight, with the ITAE index receiving the greatest emphasis, as fertilization accuracy is the core objective; thus, the optimization process prioritizes the minimization of rotational speed tracking error. Overshoot suppression ($w_2 = 0.3$) was considered the second priority, since excessive fertilizer output directly leads to material waste and must be strictly controlled. Response speed ($w_3 = 0.15$) ensures that the system can rapidly adapt to changes in operating conditions, although it is of lower priority than accuracy and overshoot. Finally, control smoothness ($w_4 = 0.05$) was included to limit abrupt variations in pulse frequency, serving as an auxiliary constraint with the lowest priority.

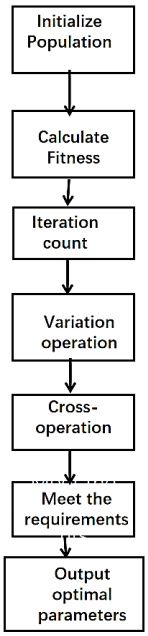

Fig. 8 – Differential Evolution Algorithm Flowchart

MATLAB simulation

As shown in Fig. 9, the PID parameters for the controlled plant were selected using an empirical trial-and-error tuning approach. The resulting parameters, Kp=17, Ki=0.02, and Kd=0.1, were used as the parameter set for the conventional PID controller. A unit-step input (amplitude of 1) was applied, the simulation duration was set to 10 s, and the sampling period was set to 100 ms. Under these conditions, the response curves of the DE-PID and the conventional PID controllers are compared in Fig. 9. To evaluate disturbance rejection performance, an instantaneous disturbance was applied to both models under the same settings, and the corresponding responses were observed and compared.

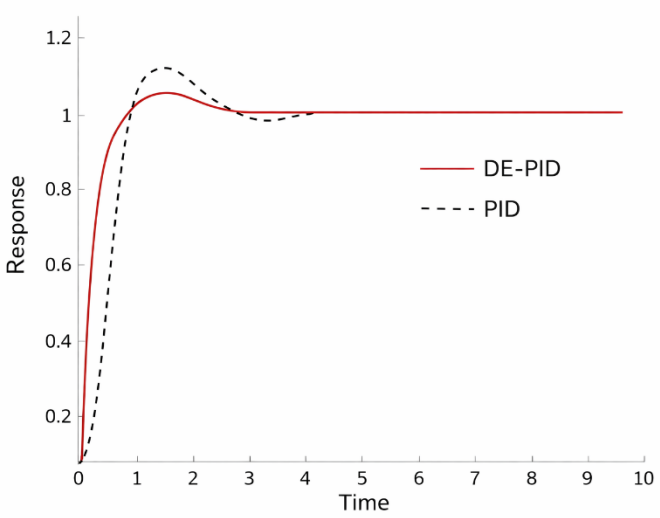

Fig. 9 – Comparison Response Curve Chart

Table 2

Comparison of Response Curves Table

Control Method	Rise /s	peak time/s	Steady-state time/s	Maximum overshoot/%
DE-PID	0.8	1.0	2.6	6.55
Traditional PID	0.9	1.2	3.8	13.25

The obtained results are comparable to those reported in previous studies on optimized PID-based agricultural control systems. Previous relevant studies have demonstrated that intelligent optimization of BP-PID parameters could improve fertilization control accuracy under variable operating conditions *(Zhu et al., 2023)*. In the present study, the DE-PID controller also showed clear advantages over the conventional PID controller, reducing the maximum relative error, average relative error, and coefficient of variation to 3.2%, 2.92%, and 0.23%, respectively. Additional related research has shown that fuzzy PID control could enhance the dynamic compensation performance of an agricultural metering system *(Chen et al., 2016).* Compared with such optimized control approaches, the DE-PID method in this study also achieved a clear improvement in transient response, with the overshoot reduced from 13.25% to 6.55% and the settling time shortened from 3.8 s to 2.6 s.

The reduction in overshoot and the improvement in system stability can be attributed to the global optimization capability of the differential evolution algorithm for the PID parameters Kp, Ki, and Kd. By optimizing these parameters under a composite objective function that incorporates ITAE, maximum overshoot, and control increment, the DE-PID controller achieves a more appropriate trade-off among rapid response, overshoot suppression, and control smoothness. In contrast to empirical PID tuning, this method avoids overly aggressive proportional action and excessive integral accumulation, thereby mitigating transient oscillation. Consequently, the system exhibits faster error attenuation, weaker sustained oscillation, and smoother control output, leading to improved transient and steady-state stability.

Field trial

To evaluate the control performance of the proposed electrically driven precision fertilization control system for the fluted-roller fertilizer applicator under complex field conditions, field trials were conducted to compare the DE-PID strategy with the conventional PID strategy at different target fertilization rates, as shown in Figs. 10–11. The trials were carried out on 20 December 2025 at the Agricultural High-Tech Zone in Dongying City, Shandong Province, China (37.25° N, 118.69° E), and comprised five experimental runs. During the tests, the tractor travel speed was maintained at 5 km/h, the fertilizer used was agricultural urea, and the rotational speed of the fertilizer applicator shaft was set to 30 r/min. The experimental setup included an Omron E6B2-CWZ6C encoder, a Siemens S7-200 SMART programmable logic controller (PLC), an 86BYG250H stepper motor, an MA860 stepper motor driver, an electronic scale, a fertilizer weighing bin, 24 V and 48 V switching power supplies, and a high-precision multimeter. The fertilizer applicator was towed by a Deutz-Fahr 1804 tractor.

Fig. 10 – Field trial process

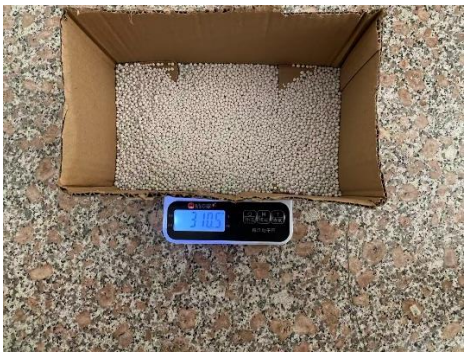

Fig. 11 – Diagram of Weighing Instruments

Performance tests were conducted to compare the fertilization error and uniformity of the fluted-roller fertilizer applicator under two different control strategies. The tractor speed was set to 5 km/h, and the rotational speed of the fertilizer applicator shaft was maintained at 30 r/min. During each test, a weighing pan placed on an electronic scale was used to measure the amount of fertilizer discharged over a period of one minute. The electronic scale had a measurement precision of 0.1 g. The relative error between the theoretical and measured fertilizer application rates, as well as the coefficient of variation, were then calculated.

$$F = \frac{M_t - M_d}{M_d} \times 100\% \quad (21)$$

where:

F is the relative error of fertilizer application rate, [%];

M_t is the measured fertilizer application rate, [g];

M_d is the theoretical fertilizer application rate, [g].

A Siemens S7-200 SMART ST40 PLC was used as the controller. The control programs corresponding to the two strategies were implemented in the PLC, and the experiments were conducted under identical conditions for each strategy. The results were subsequently compared and analyzed.

Table 3

Field Test Comparison Table

Test Number	Traditional PID Control			DE-PID Control		
	Theoretical Fertilizer Application Rate / g	Measured fertilizer application rate / g	Relative error/%	Theoretical Fertilizer Application Rate / g	Measured fertilizer application rate / g	Relative error / %
1	300	310.5	3.5	300	308.4	2.8
2	300	312.6	4.2	300	309.6	3.2
3	300	311.1	3.7	300	309.3	3.1
4	300	309.6	3.2	300	307.8	2.6
5	300	311.4	3.8	300	308.7	2.9

Under both the conventional PID controller tuned by empirical trial-and-error and the proposed DE-PID controller, the fertilizer application rates were close to the target value. With conventional PID control, the maximum relative error was 4.2%, the mean relative error was 3.68%, and the coefficient of variation (CV) of the application rate was 0.36%. Under DE-PID control, the maximum relative error was 3.2%, the mean relative error was 2.92%, and the CV was 0.23%. These results indicate that the DE-PID strategy achieves higher fertilization control accuracy than the conventional PID, demonstrating its advantages in precision fertilization control.

CONCLUSIONS

This study addressed the need for stable fertilizer discharge control in an electrically driven precision fluted-roller fertilizer applicator under complex field operating conditions. A closed-loop fertilization control system was developed, and a PID parameter optimization method was investigated. The main conclusions are as follows.

A closed-loop control system was established with a Siemens S7-200 SMART PLC as the core controller, a stepper motor as the actuator, and an incremental encoder as the feedback element, enabling real-time regulation of the fertilizer metering roller speed during field operations.

The proposed DE-PID strategy effectively overcomes the limited adaptability of empirically tuned PID parameters. MATLAB simulations showed that DE-PID reduced the maximum overshoot by 50.6% and shortened the settling time by 31.6%, resulting in significant improvements in both dynamic and steady-state performance.

Field experiments further demonstrated that DE-PID achieved a maximum relative error of 3.2%, an average relative error of 2.92%, and a coefficient of variation of 0.23%. Compared with conventional PID control, these values were reduced by 23.8%, 20.7%, and 36.1%, respectively, indicating a substantial improvement in fertilization accuracy and uniformity.

ACKNOWLEDGEMENT

This work was supported by National Key Research and Development Program of China (Project no. 2023YFD2001400), National Key R&D Program of China (Project no.2022YFE0125800).

REFERENCES

[1] Boac, J.M., Ambrose, R.P.K., Casada, M.E., Maghirang, R.G., Maier, D.E. (2014). Applications of Discrete Element Method in Modeling of Grain Postharvest Operations [J]. *Food Engineering Reviews*, Vol. 6, pp. 128-149.

[2] Cao M., Ma J. (2022). Research on improved grasshopper optimization algorithm in PID control of fuzzy neural networks (改进蝗虫优化算法在模糊神经网络 PID 控制中的研究). *Electronic Measurement Technology*, Vol. 45, no 20, pp. 74-80.

[3] Chen K., Yuan Y., Zhao B. (2022). Design of Dynamic Compensation System for Corn Seeding Position Based on Fuzzy PID Control and Analysis of Bench Test [J]. *INMATEH - Agricultural Engineering*, Vol. 67, no 2, pp. 394-405.

[4] Chen M., Wang X., Sun G., Li Y., Zhang, L. (2016). Research on Precision Sowing and Fertilization Control System for Winter Wheat (冬小麦精准播种施肥控制系统研究). *Journal of Chinese Agricultural Mechanization*, Vol. 37, no 9, pp. 24-27+42.

[5] Deng B., Shi Y. (2019). Modeling and Optimizing the Composite Prepreg Tape Winding Process Based on Grey Relational Analysis Coupled with BP Neural Network and Bat Algorithm [J]. *Nanoscale Research Letters*, Vol. 14, no 1, pp. 296.

[6] Han, C., Liu, Z., Mao, H., Ma, X., Wang, S. (2024). Design and Experiment of Variable Rate Fertilization Combined Soil Preparation Machine (棉田变量施肥整地联合作业机设计与试验). *Transactions of the Chinese Society for Agricultural Machinery*, Vol. 55, pp. 250-261+284.

[7] He, Y., Bayly, A.E., Hassanpour, A. (2018). Coupling CFD-DEM with dynamic meshing: A new approach for fluid-structure interaction in particle-fluid flows. *Powder Technology*, Vol. 325, pp. 620-631.

[8] Hou X., Li L. (2023). Predictive Filtering PID Control Based on BP Neural Network Identification (基于 BP 神经网络辨识的预测滤波 PID 控制). *Journal of Huanghe S&T University*, Vol. 25, no 5, pp. 26-31.

[9] Huang, Y., Liu, Q., Song, H., Han, T., Li, T. (2024). CMGWO: Grey wolf optimizer for fusion cell-like P systems. Heliyon, Vol. 10(14).

[10] Huang, Y., Lu, S., Liu, Q., Han, T., Li, T. (2025). GOHBA: Improved Honey Badger Algorithm for Global Optimization. Biomimetics, Vol. 10(2), p. 92.

[11] Inthiyaz, S., Nalli, R., Rakesh, T., Subbarao, K., Rajesh, V. (2021). GA based PID controller: design and optimization. *2021 6th International Conference on Inventive Computation Technologies (ICICT)*, pp. 285-289.

[12] Nan J., Chen X., Yan J. (2024). Array antenna fault detection method based on DE-GA algorithm (基于 DE-GA 算法的阵列天线故障检测方法). *Journal of Electronic Measurement and Instrumentation*, Vol.38, no.11, pp. 33-39.

[13] Sharaby N., Doroshenko A., Butovchenko A. (2019). A Comparative Analysis of Precision Seed Planters [J]. *E3S Web of Conferences*, Vol. 135, pp.1080.

[14] Umeda, M., Kaho, T., Iida, M., Lee, C.K. (2001). Effect of Variable Rate Fertilizing for Paddy Field. *2001 ASAE Annual Meeting*, pp.1-6.

[15] Wang, J., Zhou, W., Tian, L., Li, S., Zhang, Z. (2017). Virtual simulation analysis and verification of seed-filling mechanism for dipper hill-drop precision direct rice seeder. *International Journal of Agricultural and Biological Engineering*, Vol. 10, no 6, pp.77-85.

[16] Zhang J., Liu G., Hu H., Huang J. (2021). Development of bivariate fertilizer control system via independent control of fertilizing unit (排肥单体独立控制的双变量施肥控制系统研制). *Transactions of the Chinese Society of Agricultural Engineering*, Vol. 37, no 10, pp.38-45.

[17] Zhu, F., Zhang, L., Hu, X., Zhao, J., Zhang, X. (2023). Precision Fertilizer Application Control System Based on BA Optimization BP-PID Algorithm (基于蝙蝠优化 BP PID 算法的精准施肥控制系统研究). *Transactions of the Chinese Society for Agricultural Machinery*, Vol. 54, no S1, pp.135-143+171.

[18] Zhu, H., Shi, W., Guo, X., Lyu, S., Yang, R., Han, Z. (2025). Potato disease detection and prevention using multimodal AI and large language model. *Computers and Electronics in Agriculture*, Vol. 229, pp.109824.

[19] Zhu, X., Guan, J., Liu, Z., Li, Y., Yang, R. (2024). Fuzzy PID control of single chamber semi active hydro-pneumatic suspension based on GA optimization. *43rd Chinese Control Conference (CCC)*, pp.792-797.

[20] Zubrilina, E., Markvo, I., Novikov, V., Beskopylny, A., Vysochkina, L., Rudoy, D., Butovchenko, A. (2019). Precise seeding planter with automated monitoring and control system. *IOP Conference Series: Earth and Environmental Science*, Vol. 403, pp.012063.